Matter dynamics under the interaction with laser pulses in the thermoelastic & plasma regimes

V. Dimitriou[1,3], E. Kaselouris[1,2,5,6], Y. Orphanos[1,2,4], E. Bakarezos[1,2], N. Vainos[4], I. K. Nikolos[6], N. A. Papadogiannis[1,2] and M. Tatarakis[1,5]

[1]*Centre for Plasma Physics & Lasers, Technological Educational Institute of Crete (TEI), Chania & Rethymnon, Greece*

[2]*Department of Music Technology & Acoustics, Technological Educational Institute of Crete (TEI), Rethymnon, Greece*

[3]*Department of Natural Resources & Environment, Technological Educational Institute of Crete (TEI), Chania, Greece*

[4]*Department of Materials Science, University of Patras, Rio, Greece*

[5]*Department of Electronics, Technological Educational Institute of Crete (TEI), Chania, Greece*

[6]*Department of Production Engineering & Management, Technical University of Crete, Chania, Greece*

Abstract

Recent experiments performed at CPPL/TEI of Crete have generated the need of new theoretical approaches, capable of combining the governing mathematics of thermoelastic, melting and plasma regimes. A coupled physics thermal-structural transient computational model based on the Finite Element Method (FEM) is developed. Computational results are validated by experimental results obtained by dynamic imaging interferometry using nanosecond pulses for both the thermoelastic and the plasma regimes.

When low energy laser nanosecond pulses irradiate matter (below the melting threshold), the physical problem is restricted in the thermoelastic regime [1]. The raise of the laser fluence drives the temperature fields to higher levels and matter dynamics behaviour change while the limits of melting and vaporization are passed. In the ablation/plasma regime the absorbed laser energy first heats the target surface to the melting point and then to the vaporization temperature. For incident laser intensities greater than the ablation threshold a large amount of electrons, ions and excited neutrals is present in the vaporized material and may absorb the laser beam above the target surface [2]. The interaction of the laser beam with the solid and the vapor

formation above the target surface involves many physical processes, which depend on both the target's thermo-physical properties and the laser beam parameters. In our work the laser thin film-substrate interaction is studied by combining a 3D-FEM simulation, with an experimental dynamic imaging interferometry (EXP), approach. The 3D-FEM model takes into account the melting and vaporization of the mass amounts that overcome the temperature correspondent limits. The finite elements belonging to this high energy concentration area are *"killed"* so as to simulate the vaporization of the material. Plasma absorption energy is also taken into account for these elements. The experimental technique utilizes a single-longitudinal mode nanosecond laser source for both generation and recording of the sample's deformation, the generation and propagation of surface acoustic waves (SAWs).

Two experimental cases are investigated: the first corresponds to direct laser irradiation of the metal film (Fig. 1a); the second corresponds to laser irradiation on the interface of substrate-film due to the transparency of the substrate (Fig. 1.b). Both laser pulses used for the generation of SAWs (pump pulses) and for recording of the surface displacement (probe pulses), are derived from a frequency-doubled (λ=532nm) Q-switched Nd:YAG laser, having t_0 FWHM time duration of 6ns. Energies of 0.8 to 20 μJ/pulse for the first case and a fixed value of 100 μJ/pulse for the second case were used. The measurements are performed using a single pulse from the laser system, split accordingly to pump and probe, at room temperature and atmospheric pressure. Variable optical delays (Δt), are introduced between the pump and probe pulses. For the extraction of the film's surface deformation and the SAWs amplitude information an interferometric data processing software was "in-house" developed (Fig. 1.c). The technique provides a few nanometers spatial resolution vertical to the film's surface, and direct whole-field imaging with nanosecond temporal resolution [3].

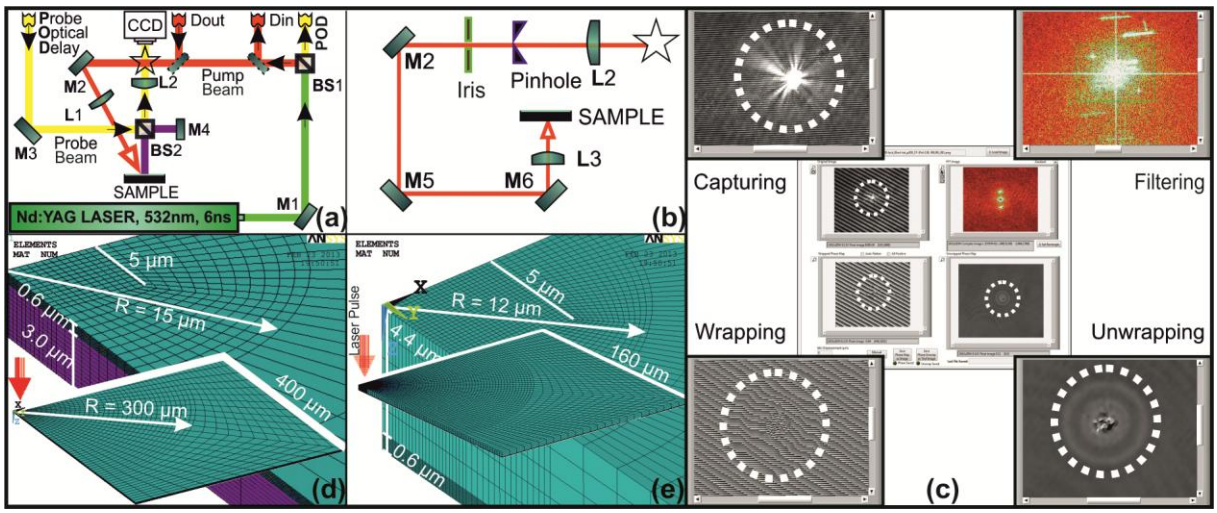

Figure 1: EXP (**a**,**b**) and FEM (**d**,**e**) setup. (**c**) Interferometric processing software main stages.

To simulate the laser matter interaction with the thin film-substrate of the two experimental cases, two 3D quarter symmetric FEM models are developed in ANSYS [4]. The models simulate a homogeneous, elastic, isotropic metal film-substrate system and its transient thermal-structural response when a single laser pulse interacts with the sample. The classical thermal conduction and the wave propagation equations are solved simultaneously. The laser beam is directed on the sample and irradiates the metalic volume from the front or the back as presented in Fig. 1.d and 1.e, respectively. A heat generation function *Q* is applied on film:

$$Q(x,y,z,t) = I_s(t)(1-R)\exp[-4\ln 2(\frac{t}{t_o})]\exp[\frac{-(x^2+y^2)}{r_o{}^2}]a\exp(-az) \quad (1)$$

where $I_s(t)$ the temporal laser irradiance at the sample, r_o the FWHM beam radius, *R* the optical reflectivity of the sample and *a* the optical absorption coefficient. For laser fluences greater than the plasma threshold, according to *Bulgakov and Bulgakova* [5], laser irradiance is attenuated due to absorption of the formed plasma. The increase in the absorption as a consequence of plasma heating is characterized by a single parameter, the density of the absorbed radiation energy E_a. Temporal laser irradiance is expressed as:

$$I_s(t) = I_0 e^{-\Lambda(t)}, \Lambda(t) = \alpha h(t) + bE_a(t) \quad (2)$$

where I_o is the incident laser intensity, Λ(t) is the optical thickness of the ablation plume, $h(t)$ is the ablation depth, and α and *b,* are time independent coefficients. Comparison [5, 6] with the experimental results allows the evaluation of coefficients *a* and *b*. The thickness of the film used is of the order of a fraction of a μm and the heat-affected zone is much smaller than the domain of the material, therefore a fine mesh is necessary to resolve temperature distribution in the film and the irradiated region. The total time solution is 60 ns. At the end of a particular solution step, if the temperature of an element is higher than the melting temperature, phase change occurs, by considering the latent heat of melting L_m in the model. Ablation occurs when the temperature of the elements is higher than the boiling temperature and in this case the latent heat of vaporization L_v is used. Material removal is achieved by the *"killing*"of the elements [6].

Temperature dependent properties of Au thin film and the material properties of BK7 glass are used in the simulations [7]. For the direct irradiation of the thin film substrate, pump laser fluences ranging from 0.1 to 5.0 J/cm^2 were used to investigate the thermoelastic and the ablation regime. In Figs 2.a and 2.b, the bulge deformation and SAW generation for the EXP and FEM are shown for laser fluence 0.54 J/cm^2 and Δt=28 ns. The bulge deformation is EXP and FEM found ~30 nm and ~23 nm, correspondingly. The SAW is EXP observed ~55 μm far from the epicenter and normally displaced ~1.5 nm. FEM resulted to ~47 μm distance far from the epicenter and ~1nm normally displaced. In Fig. 2.c pump laser fluence of 3.9 J/cm^2 is used.

The FEM results compared to EXP lead to *a* and *b* values evaluation ($1x10^6$ and $1x10^{-4}$, respectively). The simulation is performed again with Eq.2 activated. The dynamic response of the metal film (crater and SAWs generation and propagation) may be clearly observed for both EXP and FEM approaches at Δt=25 and 33 ns. For the case of the indirect irradiation of the same sample, great pump laser fluence is used (30 J/cm^2). The generated crater walls have a diameter of ~40 μm for EXP and ~35 μm for FEM (Figs 1.d. and 1.e). Their vertical displacement is ~60 nm for both EXP and FEM. The first SAW has a value of 3 nm for both EXP and FEM and is observed ~50 μm and ~45 μm far from the epicenter for EXP and FEM respectively.

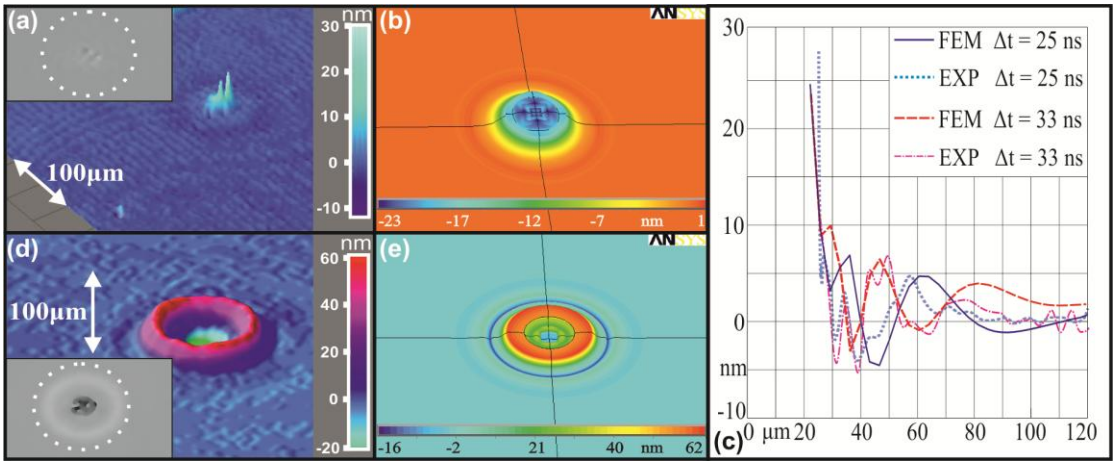

Figure 2: EXP (**a,d**) vs FEM (**b,e**) results for Δt=28ns. (**c**) Comparison of EXP and FEM results

The EXP results compared to FEM are found to be in a very good agreement. The results demonstrate that the combination of the integrated FEM model and the EXP method is capable to fully describe the transient surface deformations in 3D and in every regime, in such material systems. Since the mass reduction due to ablation and the temporal distribution are computed in every time-step, the developed FEM model may be further used to include the liquid phase of the melted material and its ionization by the help of CFD and MHD computational methods.

References

[1] S. J. Davies *et al*., J. Phys. D Appl. Phys. **26**, 329 (1993).

[2] S. Amoruso, Appl. Phys. A **69**, 323 (1999).

[3] Y. Orphanos *et al*., Microelectron. Eng. http://dx.doi.org/10.1016/j.mee.2013.03.146 (2013).

[4] ANSYS, "Theory Reference for the Mechanical APDL and Mechanical Applications", ANSYS Inc., Southpointe, USA (2009).

[5] A. V. Bulgakov and N. M. Bulgakova, Quantum Electron. **29**, 433 (1999).

[6] N. A. Vasantgadkar, U. V. Bhandarkar, and S. S. Joshi, Thin Solid films **519**, 1421 (2010).

[7] http://www.engineeringtoolbox.com & http://www.efunda.com (last accessed June 2013).

This research has been co-funded by the European Union (European Regional Development Fund – ERDF) and Hellenic national funds through the Operational Programme "Competitiveness and Entrepreneurship" of the National Strategic Reference Framework (NSRF) 2007-2013 – Funded Research Program: National Research Infrastructure for HiPER.